Virus Research 265 (2019) 10–19

Contents lists available at ScienceDirect

Virus Research

journal homepage: www.elsevier.com/locate/virusres

Molecular characterization of virus-derived small RNAs in *Nicotiana benthamiana* plants infected with tobacco curly shoot virus and its β satellite

Gentu Wu[a], Qiao Hu[a], Jiang Du[a], Ke Li[a], Miao Sun[a], Chenchen Jing[a], Mingjun Li[a], Junmin Li[b], Ling Qing[a,*]

[a] Chongqing Key Laboratory of Plant Disease Biology, College of Plant Protection, Southwest University, Chongqing, 400716, China
[b] Institute of Plant Virology, Ningbo University, Ningbo, 315211, China

ARTICLE INFO

Keywords:
Tobacco curly shoot virus
Virus-derived small interfering RNAs
Deep sequencing technology
Transcripts
Functional annotation

ABSTRACT

Tobacco curly shoot virus (TbCSV) is a monopartite DNA virus of the genus *Begomovirus*, which causes leaf curl symptoms in tobacco and tomato. The β satellite of TbCSV (TbCSB induces more severe symptoms and enhanced virus accumulation when co-infects the host plants with TbCSV. Small interfering RNAs derived from virus (vsiRNAs) induce disease symptoms and promote virus invasion by target and guide the degradation of host transcripts The vsiRNAs derived from TbCSV and TbCSV + TbCSB remained to be explored to elucidate the molecular mechanism of symptoms development in plants. In the present work, two libraries of small RNA from TbCSV-infected and TbCSV + TbCSB-infected *N. benthamiana* plants were constructed and the vsiRNAs in both samples shared the same characteristics. The size of the vsiRNAs ranged from 18 to 30 nucleotides (nt), with most of them being 21 or 22 nt, which accounted for 29.11% and 23.22% in TbCSV plants and 29.39% and 21.82% in TbCSV + TbCSV plants, respectively. The vsiRNAs with A/U bias at the first site were abundant in both the TbCSV-treated and TbCSV + TbCSB-treated plants. It is discovered that the vsiRNAs continuously, but heterogeneously, distributed through bothe the TbCSV and TbCSB sequences. And the distribution profiles were similar in both the treatments such as mainly in the overlapping region of the *AC2/AC3* coding sequences. The host transcripts targeted by vsiRNAs were predicted, and the targeted genes were found to be involved in varied biological processes. It is indicated that the presence of TbCSB does not significantly affect the production of vsiRNAs from TbCSV in plants, the distribution hotsopt of TbCSV vsiRNAs could be useful in designing effective targets for TbCSV resistance exploiting RNA interference.

1. Introduction

Plant microRNAs (miRNAs), play vital roles in controlling development and productivity. For examples, miR156 and miR172 act as major factors in the plant growth and propagation (Teotia and Tang, 2015; Xie et al., 2006; Sha et al., 2014), and miR164 modulates leaf development by regulating growth, which determines leaf shape (Byrne, 2012). Plant miRNAs also play roles in plant defense against pathogens by regulating the expression of resistance genes (Shivaprasad et al., 2012; Yin et al., 2015) and genes associated with viral symptoms (Wang et al., 2018). For example, miR6019-mediated innate immunity during plant growth is regulated by the expression level of NLR (Deng et al., 2018), and osa-miR171b contributes to stunting and yellowing symptoms in rice stripe virus (RSV)-infected rice plants (Tong et al., 2017).

Pants viruses infection usually cause production of small interfering RNAs derived from the viruses genomes in host plants. These virus-derived small interfering RNAs (vsiRNAs), which range in length from 21- to 24- nucleotides (nt), are generated by Dicer-like (DCL) proteins that recognize and cleave the double-stranded viral RNA (dsRNA) and base-paired single-stranded RNA (ssRNA) (Hamilton and Baulcombe, 1999; Molnar et al., 2005). In plants, DCL4 and DCL2 are most important DCLs for the production of 21- and 22-nt vsiRNAs, respectively (Bouche et al., 2006; Donaire et al., 2008; Garcia-Ruiz et al., 2010). The antiviral immunity is mainly conferred by DCL4-dependent 21-nt vsiRNAs with DCL2 as a surrogate (Bouche et al., 2006; Brodersen et al., 2008). Some vsiRNAs are loaded into the Argonaute (AGO)-containing complexes to inactivate both viral genomes and in some cases the host mRNAs (Miozzi et al., 2013; Shimura et al., 2011; Jaubert et al., 2011; Zhu et al., 2011). Additionally, the vsiRNAs can be amplified by RNA-

* Corresponding author.
E-mail addresses: wugtu@163.com (G. Wu), 517793064@qq.com (Q. Hu), 624591943@qq.com (J. Du), 360731681@qq.com (K. Li), 445879215@qq.com (M. Sun), 1210186161@qq.com (C. Jing), lmj603@163.com (M. Li), 65222017@qq.com (J. Li), qling@swu.edu.cn (L. Qing).

https://doi.org/10.1016/j.virusres.2019.02.017
Received 25 November 2018; Received in revised form 25 February 2019; Accepted 28 February 2019
Available online 01 March 2019
0168-1702/

dependent RNA polymerases (RDRs), which help to enhance their functions. This process leads to production of secondary vsiRNAs that further reinforce the activity of the RNA silencing. Host-encoded RDRs including *RDR1*, *RDR2* and *RDR6* are responsible for this amplification process (Csorba et al., 2015; Wang et al., 2010). These vsiRNAs are recruited into the RNA-induced silencing complex by the AGO proteins, and this process is conducted by their 5′-terminal nucleotides (Brodersen et al., 2008; Fang and Qi, 2016; Mi et al., 2008).

It is well known that vsiRNAs target and degrade viral RNAs in plants, which benefits the host as a protection mechanism against viral infection. Recently, reports have shown that some vsiRNAs guide the degradation of host transcripts at the post-transcriptional level by base-pairing mechanisms to induce disease symptoms and promote virus invasion (Shi et al., 2016; Shimura et al., 2011; Smith et al., 2011). The vsiRNA from the Y satellite of cucumber mosaic virus (CMV) cleaves *Ch1I* mRNA in *N. benthamiana* and causes yellowing symptoms (Shimura et al., 2011; Smith et al., 2011). The vsiRNA from RSV RNA4 targets host *eukaryotic translation initiation factor 4 A* (*eIF4 A*) which leads to leaf curling and wilting (Shi et al., 2016). Furthermore, vsiRNAs from CMV target abundant host genes that participate in metabolic processes, cellular processes, and single-organism processes, as shown by analysis using Gene Ontology (GO) annotation, and genes that are related to metabolic activities, as shown by analysis using the Kyoto Encyclopedia of Genes and Genomes (KEGG) (Qiu et al., 2017). Southern rice black-streaked dwarf virus (SRBSDV)-derived vsiRNAs, most of which are 21- or 22- nt in length, target a series of rice genes related to host defense, pathogenesis, and symptomology (Xu and Zhou, 2017). Moreover, many plant factors can be targeted by vsiRNAs, such as resistance proteins, kinase proteins, transcription factors, F-box proteins, and pathogen-related proteins (Miozzi et al., 2013).

Tobacco curly shoot virus (TbCSV), a member of the genus *Begomovirus*, consists of DNA (TbCSV) and DNA-β (tobacco curly shoot β satellite, TbCSB) and is transmitted exclusively by whitefly (*Bemisia tabaci*) as vector in tobacco, tomato, and weeds. Leaf curl disease caused by co-infection of TbCSV and TbCSB (TbCSV + TbCSB) complex in tobacco and tomato have been resulted in great economic losses. TbCSV is a circular single-stranded DNA (ssDNA) helper virus of approximately 2.7 kilonucleotides (knt) that encodes the *AV1*, *AV2*, *AC1*, *AC2*, *AC3*, and *AC4* genes. TbCSB is ssDNA of about 1.3 knt and encodes the βC1 gene. Most begomoviruses require a β satellite to induce typical disease symptoms (Mansoor et al., 2003; Tao and Zhou, 2008). However, the TbCSV + TbCSB disease complex differs from other begomovirus/β satellite disease complexes in its pathogenicity and its role in regulating disease symptoms. TbCSV alone is able to induce severe symptoms, such as upward leaf curling, in tomato and tobacco plants. However, TbCSB was found to intensify the symptoms induced by TbCSV in *Nicotiana* spp., while the symptoms changed to downward leaf curling (Ding et al., 2009; Li et al., 2005). Although the functions of the viral genes are well known, few studies have focused on vsiRNA profiles from geminiviruses, especially TbCSV/TbCSB pathotypes. With the development of deep sequencing technology, an increasing number of vsiRNAs have been identified and the functions of their target genes have been characterized (Moyo et al., 2017; Qiu et al., 2017; Xu and Zhou, 2017). In this study, we used small RNA deep sequencing to comparatively analyze the vsiRNA profiles of *Nicotiana benthamiana* plants exhibiting the typical symptoms upon inoculation infection with TbCSV or TbCSV + TbCSB.

2. Material and methods

2.1. Plant materials and viral infiltration

Nicotiana benthamiana (*N.b*) plants were grown in a greenhouse at 25 °C under a 16-h light/8-h dark photoperiod. Infectious clones of the TbCSV isolate (Y35 A) and its associated β satellite, TbCSB (Y35B), were used in virus infiltration. *N.b* plants were infiltrated with the infectious clone of TbCSV (TbCSV alone infected named TbCSV treatment) or TbCSV + TbCSB (TbCSV plus TbCSB infected named TbCSV + TbCSB treatment) at the five-leaf stage and mock-inoculated plants were used as control. DNA was extracted by the cetyltrimethylammonium bromide (CTAB) method. Systemically-infected leaves were collected at 20 days post-inoculation (dpi). The presence of TbCSV and TbCSB was detected by PCR. Specific primers for the *AV1* and βC1 genes were: AV1 F (5′-ATGTCGAAGCGTCCAGCAG-3′), AV1 R (5′-TTAATTTGTTACGGAATCATAGA-3′), βC1 F (5′-ATGACAATTAAAT ACAACAACAAG-3′), and βC1 R (5′-TCATACATTAGCTATTGTCCC-3′).

2.2. Small RNA library construction and sequencing

To obtain small RNA libraries from TbCSV- and TbCSV + TbCSB-infected plants, RNA from the virus-infected and mock-inoculated plants (three seedlings per treatment were used as biological replicates) were extracted with TRIzol reagent (Ambion, Austin, TX, USA, product no. 15596026) according to the manufacturer's instructions. RNA was quantified using agarose gel electrophoresis (AGE) and a NanoDrop spectrophotometer. RNA was size-fractionated by 15% polyacrylamide gel electrophoresis (PAGE), and small RNAs in the range of 18 to 30 nt were enriched. Then, the purified small RNAs were ligated with 5′ and 3′ adaptors to the termini. The ligated small RNAs were used as templates for synthesis of cDNAs. These libraries were sequenced on the Solexa Illumina platform (Novogene Company, Beijing, China). Clean reads were used directly for further bioinformatic analysis.

2.3. Bioinformatic analyses of small RNAs

For analysis of small RNAs, low quality and junk sequences, including transfer RNAs (tRNAs), ribosomal RNA (rRNAs), etc., were removed using the FASTX-Toolkit software (http://hannonlab.cshl.edu/fastx_toolkit) (Li et al., 2016a). Clean small RNA sequences were collected and subjected to BLAST analysis against the TbCSV genome (NCBI accession No.: AJ420318) and the TbCSB genome (NCBI accession No.: AJ421484). The small RNA sequences 18–30 nt in length were selected as candidate vsiRNAs. The output files were searched and summarized using customized scripts in BowTie software (http://bowtie-bio.sourceforge.net) to identify those with an exact match for TbCSV and TbCSB over their entire length. This process allowed us to identify the sequences that exactly matched TbCSV and TbCSB in the range of 18–30 nt. Further statistical analyses and summaries were performed using Microsoft Excel 2013 software.

2.4. Reverse transcription PCR (RT-PCR)

For analyses of the vsiRNAs, small RNA was extracted from the TbCSV- infected (20 dpi) and mock-inoculated plants using RNAiso reagent (TaKaRa Bio, Inc., Dalian, China, product no. 9753 A) and cDNA was synthesized using TranScript miRNA First-Strand cDNA Synthesis SuperMix (Transgen Biotech, Beijing, China, product No. AT351) following the manufacturer's instructions. PCR was carried out using TransTaq DNA Polymerase High Fidelity (Transgen Biotech, Beijing, China, product no. AP131). The primers used were a vsiRNA-specific forward primer and a universal primer, the sequences of which were listed in Additional file 1: Table S1. Small RNAs were quantified using AGE, purified, cloned into pGEM-T-easy vectors (Promega, USA, product no. R6881), and sequenced.

2.5. Prediction and annotation of target genes

To obtain the targets of the vsiRNAs, 19 reads vsiRNAs listed in Additional file 1: Table S1 were performed using the online analysis tool psRNATarget (http://plantgrn.noble.org/psRNATarget). The predicted target genes were subjected to BLAST alignment. GO annotation was carried out using BLAST2GO software. KEGG classification of the

predicted target genes was conducted using KEGG Mapper-Annotate Sequence by FBlastKOALA, which is available on the Kyoto Encyclopedia of Genes and Genomes website (https://www.kegg.jp/kegg/tool/annotate_sequence.html) (Xu and Zhou, 2017).

2.6. Real-time quantitative PCR (RT-qPCR)

To analyze the expression of vsiRNA targets, total RNA was extracted from TbCSV- infected plants and mock-treated plants using TRIzol reagent (Ambion, Austin, TX, USA, product no. 15596026) according to the manufacturer's instructions. cDNA was synthesized from 1 μg of total RNA in a volume of 20 μL using the PrimeScript RT Reagent Kit (TaKaRa Bio, Inc., Dalian, China, product no. RR037 A). qPCR was performed using KOD SYBR qPCR mix (Toyobo, Osaka, Japan, product no. QKD-201) with the Bio-Rad iQ5 Real-Time PCR system with gene-specific primers (Additional file 2, Table S2). *Glyceraldehyde-3-phosphate dehydrogenase* (*GAPDH*) was used as internal control gene. All RT-qPCR reactions were performed in triplicate, each with three biological replicates, and repeated three times. The number of transcripts based on Ct values was determined using the ΔΔCt method.

3. Results

3.1. TbCSB enhances the accumulation of TbCSV siRNAs

We compared deep sequencing data and the percentages of vsiRNA reads mapping against viral genomes in TbCSV- and TbCSV + TbCSB-infected *N. benthamiana* (Table 1). 12,317,577 and 13,896,237 clean reads in total, were obtained from small RNA libraries constructed from these two samples, respectively, collected at 20 dpi. Among them, 217,272 vsiRNA reads and 32,192 unique sequences from the TbCSV-infected samples were mapped to the TbCSV genome. Then, 1,165,882 reads and 87,315 unique sequences from the TbCSV + TbCSB- infected samples were mapped to the TbCSV and TbCSB genome, among of them 1,151,490 reads and 82,497 unique sequences were mapped to the TbCSV genome, and 14,392 reads and 4,818 unique sequences were mapped to the TbCSB genome. The TbCSV- derived vsiRNAs shared 1.76% (total) and 1.32% (unique) of sequences compared to the small RNA library of the TbCSV- infected sample. However, the small RNAs from TbCSV + TbCSB- infected samples accounted for 8.39% (8.29% +0.10%) (total) and 1.53% (0.45%+0.08%) (Unique) of sequences in the TbCSV + TbCSB small RNA library (Table 1). Results showed that the total number of vsiRNAs from TbCSV + TbCSB- infected plants was significantly greater than that from TbCSV- infected plants. Based on these analyses, we hypothesize that TbCSB, the β satellite of TbCSV, may influence the accumulation of small RNAs, while TbCSB encodes a βC1 protein, which is a suppressor of RNA silencing.

3.2. TbCSB doesn't alter the characteristics of TbCSV siRNA

In both small RNA libraries, the most dominant vsiRNA size was 22-nt, followed by 21- nt and 24- nt (Fig. 1a). In TbCSV- infected *N. benthamiana*, the vsiRNAs that are 22-, 21-, and 24- nt in length accounted for 65.39% of total unique viral reads, while the 22- nt vsiRNAs were clearly the most dominant, accounting for 29.11% of total unique viral reads. VsiRNAs of the 21- and 24- nt classes accounted for 23.22% and 13.06% of total unique viral reads, respectively. Moreover, the vsiRNAs derived from TbCSV in TbCSV + TbCSB- infected plants, shared the same size distribution, with the 22-, 21- and 24- nt classes accounting for 29.39%, 21.82%, and 12.65% of total unique viral reads, respectively. For vsiRNA derived from TbCSB-infected plants, the 22- nt class was also the most dominant, accounting for 27.6% of total unique viral reads, followed by the 21- and 24- nt classes, accounting for 19.45% and 18.71% of total unique viral reads, respectively. Thus the proportion of 24- nt vsiRNAs from TbCSB-infected plants was higher than that from plants infected with TbCSV alone. These results suggest that the *N. benthamiana* homologs of DCL2 and DCL4 may be the predominant DCL components with respect to TbCSV siRNAs and their biogenesis, and that TbCSB did not affect the function of DCL2 and DCL4. In addition, we detected less 23- and 24-nt vsiRNAs, suggesting that the role of DCL3 in the biogenesis of TbCSV- specific vsiRNAs in *N. benthamiana* is minor.

Previous studies have indicated that loading of vsiRNAs onto particular AGO complexes is biased and dictated by the 5′-terminal nucleotides of the vsiRNAs. For further insight into vsiRNA biogenesis and sorting, we analyzed 21- and 22-nt vsiRNAs. The bioinformatics data revealed that vsiRNAs (21- and 22- nt) with a uracil (U) at their 5′-termini were the most abundant in both the TbCSV- and TbCSV + TbCSB- infected plants, followed by adenine (A), cytosine (C), and guanine (G), respectively (Fig. 1b). The 21(+)-nt, 21(–)-nt, 22(+)-nt, and 22(–)-nt vsiRNAs of 21- and 22- nt vsiRNAs from TbCSV- infected plants had a 5′-terminal U, accounting for 13.96%, 8.68%, 20.01%, and 11.42% of the total, respectively. The vsiRNAs derived from TbCSV in TbCSV + TbCSB- infected plants, the 5′-terminal U accounted for 13.36%, 6.16%, 20.32%, and 8.96% of the total, while in the vsiRNAs derived from TbCSB in TbCSV + TbCSB- infected plants, the 5′-terminal U accounted for 14.00%, 6.89%, 20.44%, and 9.89%, respectively. These results show that in both TbCSV- and TbCSV + TbCSB- infected plants, the 5′-terminal nucleotide of vsiRNAs was biased toward U, and the β satellite of TbCSV did not change the 5′-terminal nucleotide preference of vsiRNAs.

3.3. TbCSB influences the distribution profile of vsiRNAs in the viral genome

To investigate the frequency distribution of vsiRNAs in the TbCSV and TbCSB genomes in the TbCSV- and TbCSV + TbCSB- infected plants, we constructed single-base resolution maps of all redundant vsiRNAs along the genomes using BowTie software tools. The mapping patterns of vsiRNAs of two size classes (21- and 22- nt) were determined. The results showed that the most abundant vsiRNAs were mainly located within open reading frames (ORFs) of TbCSV and TbCSB (Fig. 2). Regions highly abundant in vsiRNAs were located in the positive strand of the AV1-encoding region and in the negative strand of the AC2/AC3- and βC1-encoding region, while less vsiRNAs mapped to the untranslated region (UTR). Furthermore, normalized reads (reads per million reads, RPM) analysis showed that the vsiRNAs read from TbCSV- infected samples were much less abundant than those from TbCSV + TbCSB- infected plants (Fig. 2a, b). For most of the vsiRNAs in TbCSV- infected plants, the normalized reads were between 100 and 200 RPM. The normalized reads were over 500 RPM in TbCSV +

Table 1
Total number of small RNAs reads from TbCSV mapped to viral genome.

Virus	Treatment	Tissue	Total reads	Unique reads	Total vsiRNAs reads (plus/negative)	Unique viRNAs reads (plus/negative)	% in total	% in unique
TbCSV	TbCSV	Leaf	12,317,577	2,438,165	217,272(140,260/77,012)	32,192(18,262/13,930)	1.76%	1.32%
TbCSV	TbCSV + TbCSB	Leaf	13,896,237	5,675,863	1,151,490(878,758/272,732)	82,497(51,550/30,974)	8.29%	1.45%
TbCSB					14,392(9,326/5,066)	4,818(2,747/2,071)	0.10%	0.08%

plus: vsiRNAs from viral positive strand; negative: vsiRNAs from negative strand.

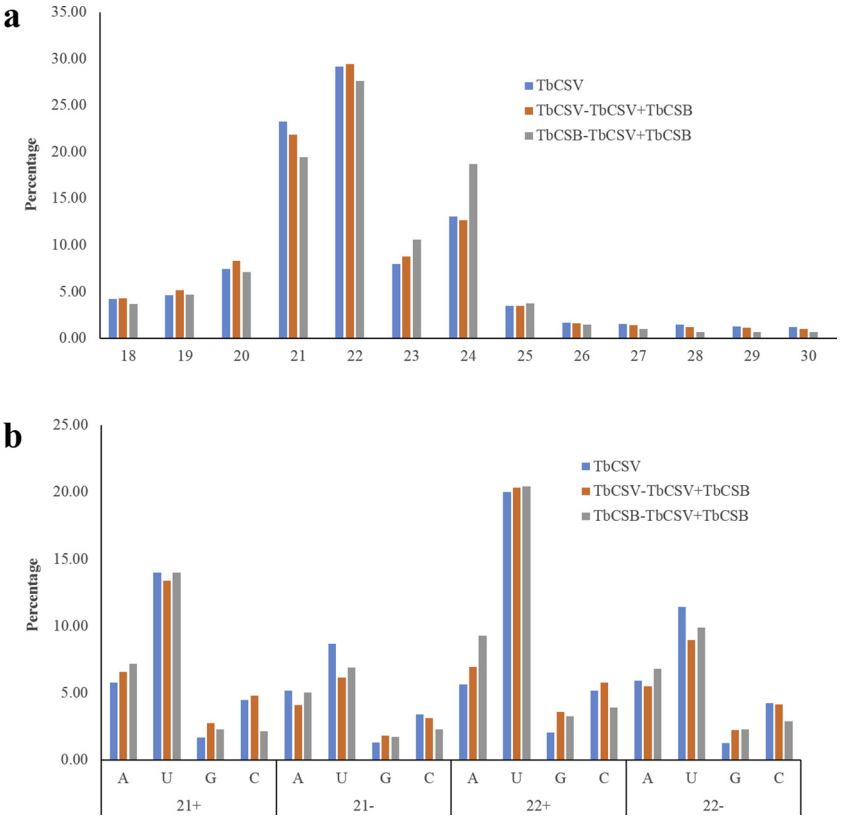

Fig. 1. Characterization of virus-derived siRNAs (vsiRNAs) from TbCSV- infected plants at 20 days post-inoculation (dpi). (a) Size distribution of total reads. (b) Percentage frequencies of different 5′-terminal nucleotides in the identified vsiRNAs.

TbCSB- infected plants. In addition, the normalized reads of vsiRNAs derived from TbCSB were about 10 RPM (Fig. 2c).

Additionally, we analyzed the hotspots of vsiRNAs. Single-base resolution maps of all redundant vsiRNAs along the genomes were constructed using Bowtie tools, the mapping patterns of 18- to 24- nt vsiRNAs were determined, and the predominance of vsiRNAs within hotspots was based on F-values (> 100) and P-values of coverage using analysis of variance (ANOVA). The results showed that all the hotspots were related to protein coding regions in the genome in both TbCSV- and TbCSV + TbCSB- infected samples. In total, 49 vsiRNA hotspots were identified in TbCSV- infected plants (Fig. 3a), with 25 (51%) of the hotspots in the positive strand and 24 (49%) of the hotspots in the negative strand. However, 55 hotspots were identified in the TbCSV genome in TbCSV + TbCSB- infected sample, including 21 (38%) of the hotspots in the sense strand and 34 (62%) of the hotspots in the antisense strand. TbCSB contained 17 hotspots (the sense and antisense strands had 7 and 10 hotspots, respectively) in TbCSV + TbCSB- infected plants (Fig. 3b, c). These results indicate that the same sites on the viral genome may be recognized and cleaved by DCL2 and DCL4, and that TbCSB may affect their function at some level.

3.4. TbCSB enhances TbCSV gene expression

To investigate the influence of TbCSB on the production of vsiRNAs in *N. benthamiana*, we compared the expression levels of viral genes between TbCSV- and TbCSV + TbCSB- infectted plants at 20 dpi using RT-qPCR (primers were shown in Additional file 1: Table S2.). The expression levels of the helper virus genes were significantly higher than that of the β satellite βC1 gene (Additional file 3: Figure S1.). In both the TbCSV- and the TbCSV + TbCSB- infected samples, the expression levels of *AV1* and *AV2* were significantly higher than those of *AC1*, *AC2*, *AC3*, and *AC4* (Fig. 4a). The expression levels of *AC3* and *AC2* were similar in TbCSV + TbCSB-infected samples; however, the expression level of *AC3* was slightly higher than that of *AC2* in TbCSV-infected plants. Compared to the TbCSV- infected plants, *AV1*, *AV2*, *AC1*, *AC2*, and *AC4* were upregulated by the presence of TbCSB, but there were no significant differences in the expression levels among different genes (Fig. 4a). This suggests that TbCSB induces the accumulation of TbCSV to some extent.

3.5. Induction NbRDRs expression in TbCSV- infected plants

To investigate the influence of TbCSV and TbCSB infection on the vsiRNA synthesis pathway, we compared the expression levels of NbRDRs among the TbCSV- infected, TbCSV + TbCSB- infected, and mock-inoculated plants at 20 dpi using RT-qPCR. *NbRDR1m* (mutated RNA-dependent RNA polymerase 1 allele of *N. benthamiana*) expression was significantly upregulated and *NbRDR2* and *NbRDR6* expression levels were slightly upregulated by TbCSV + TbCSB infection compared with the mock-inoculated control, while *NbRDR1m* and *NbRDR2* were slightly upregulated in the TbCSV- infected compared with the mock-inoculated control (Fig. 4b). The expression of *NbRDR1m* in TbCSV + TbCSB- infected plants was significantly higher than that found in the TbCSV- infected plants, but there were no differences in the expression levels of *NbRDR2* and *NbRDR6* between the two samples (Fig. 4b). These results suggest that TbCSV induces the expression of NbRDRs, but TbCSB does not affect the expression of NbRDRs.

3.6. TbCSV siRNAs were cloned

To determine whether the vsiRNAs were derived from RNA transcription units, some vsiRNAs were cloned using RT-PCR. We selected 55 small RNAs from TbCSV with over 2000 reads for further analysis. The results showed that 19 vsiRNAs, accounting for 34.5% of the vsiRNAs analyzed (Table 2). Furthermore, the number of reads of these 19 vsiRNAs was over 2000, and most (78.9%) of them were derived

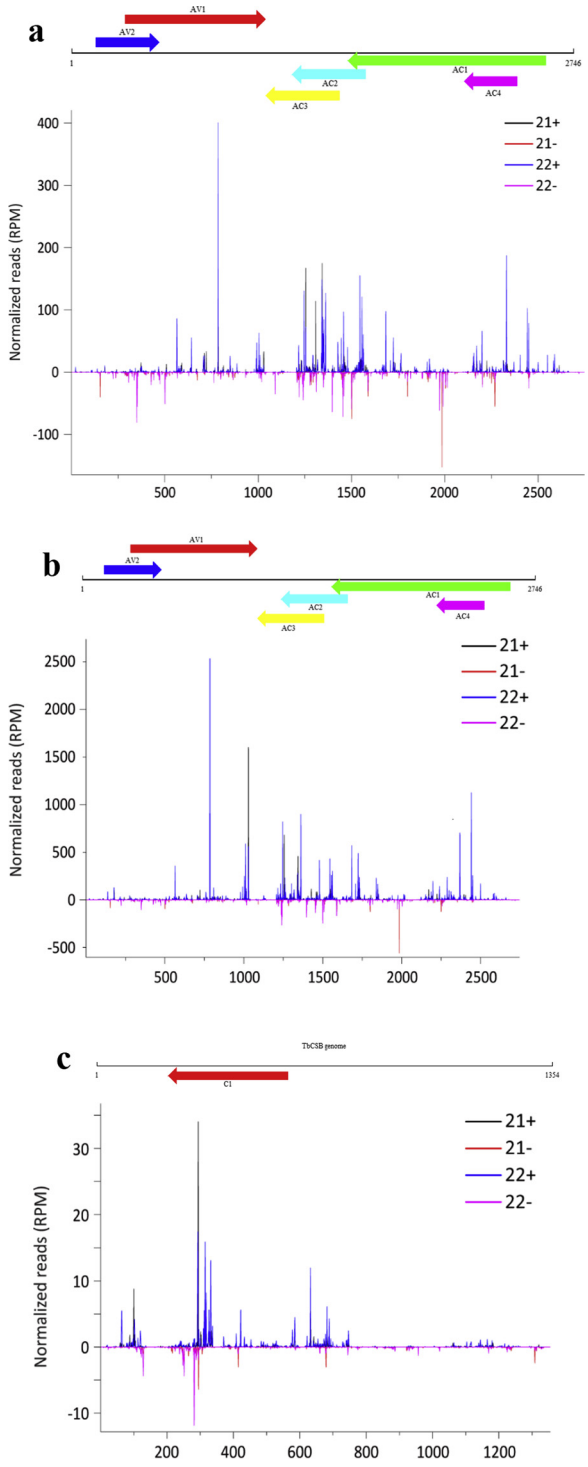

Fig. 2. The distribution of siRNAs on the TbCSV (a and b) and TbCSB (c) genomes. Single-base resolution maps of all redundant viral derived siRNAs along the genomes were constructed using Bowtie tools, the mapping patterns of vsiRNAs of 18- to 24-nt were clarified. The X axis represents the length of the genome, and the Y axis reprensents the number of siRNAs. Hotspots accumulating vsiRNAs at precise positions are indicated by V1-V3 and S1-5 (> 10,000 reads), respectively. (V means hotspot at viral strand, S means hotspot at antisense strand) (a) The distribution of siRNAs on TbCSV genome in TbCSV- infected plants. (b) The distribution of siRNAs on TbCSV genome in TbCSV + TbCSB- infected plants. (c) The distribution of siRNAs onTbCSB genome in TbCSV + TbCSB- infected plants.

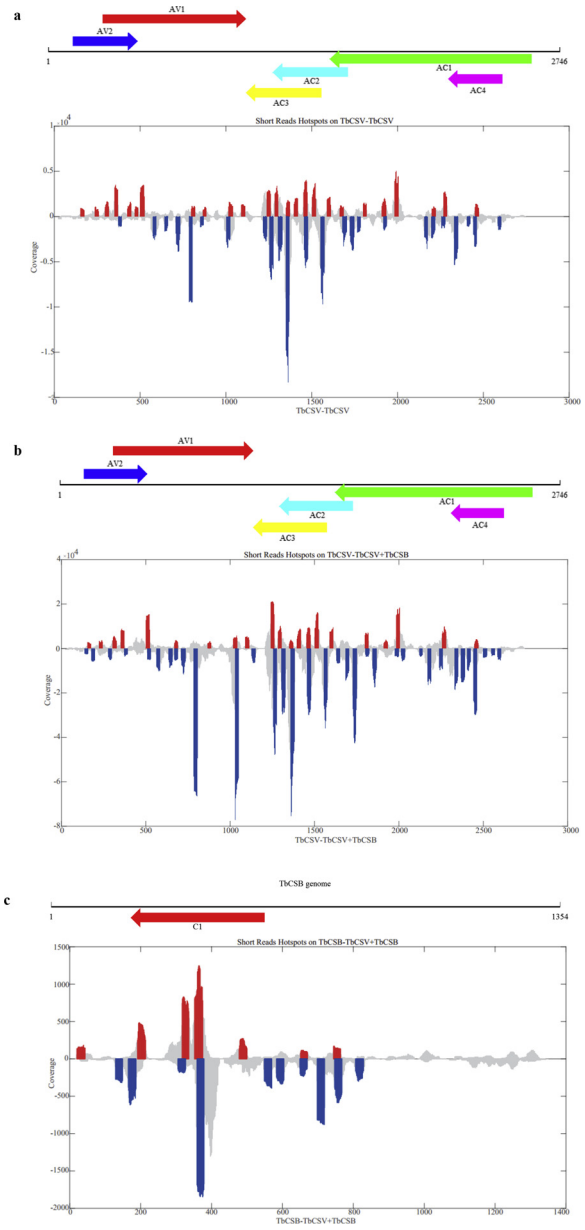

Fig. 3. The hotspots of vsiRNAs derived from the viral genome. VsiRNAs were predominated within hotspots according to F-values (> 100) and its P-values of coverage using ANOVA. The siRNAs are shown in orange above (positive strand) and in blue below (negative strand) the horizontal line. (a) The hotspots of vsiRNAs derived from the TbCSV genome in TbCSV- infected plants. (b) The hotspots of vsiRNAs derived from the TbCSV genome in TbCSV + TbCSB- infected plants. (c) The hotspots of vsiRNAs derived from the TbCSB genome in TbCSV + TbCSB- infected plants.

from negative strand. We also carried out RT-PCR to clone the 14 vsiRNAs, the results showed all of them can be cloned from the small RNA cDNA, and the sequenced results were shown in the Additional file 4: Figure S2. These results suggest that vsiRNAs derived from TbCSV are predominantly produced by direct cleavage in the viral mRNAs.

3.7. Targets of TbCSV- derived small RNAs

To gain further insight into the function of the vsiRNAs, we used the psRNATarget server to explore the *N. benthamiana* genes putatively targeted by TbCSV- derived vsiRNAs. Of the large number of vsiRNAs that were sequenced, 55 small RNAs from TbCSV with over 2000 reads were selected for further analysis. Only 21 vsiRNAs (accounting for

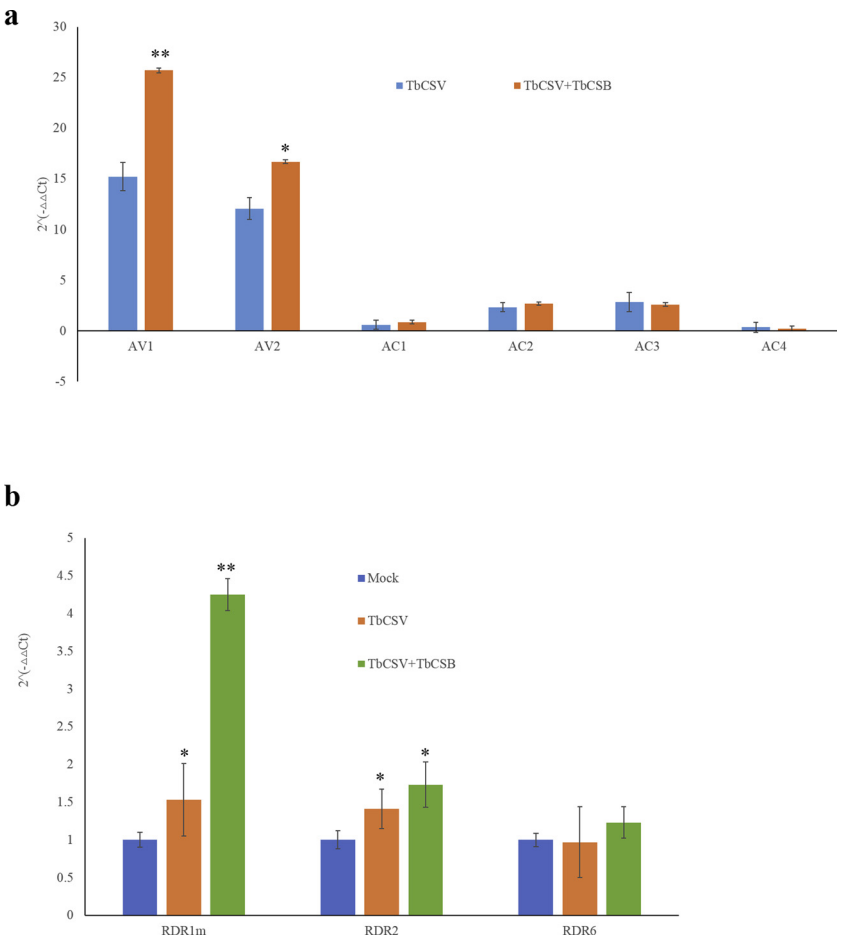

Fig. 4. Expression levels of viral genes and NbRDRs. (a) The relative expression levels of viral genes in TbCSV- and TbCSV + TbCSB- infected plants. Asterisks indicate statistically significant differences compared with each other. The single and double asterisks indicate significance levels of 0.05 and 0.01 respectively. (b) The relative expression levels of NbRDRs in TbCSV- and TbCSV + TbCSB- infected plants. Asterisks indicate statistically significant differences compared with Mock. The single and double asterisks indicate significance levels of 0.05 and 0.01 respectively.

38.2%) were predicted to target host genes, included the 19 vsiRNAs were derived from viral mRNAs. Thus, 19 unique vsiRNAs were predicted to target 117 *N. benthamiana* annotated genes (Additional file 5: Table S3). The results showed that a number of annotated targets were related to disease or stress responses, cellular regulation, biosynthesis, and metabolism.

Using BLAST2GO software, we subjected 117 target genes (Additional file 5: Table S3) to perform GO analysis. The target coding transcripts for vsiRNAs were classified into three GO categories (cellular components, molecular functions, and biological processes) and 20 subcategories (Fig. 5). The two most highly represented GO terms were “binding” and “catalytic activity” under the molecular function category, constituting 41% of the annotated genes. The two most abundant GO terms under the biological process were related to metabolic processes and cellular processes, representing 22% of the classified targets. Moreover, we conducted KEGG pathway analysis for the

Table 2
VsiRNAs were derived from viral genes.

siRNA name	Start	End	Strand	Length	AverCov	siRNA sequence (5’ to 3’)	Position
Y35A1	1240	1261	+	22	19555.23	GUGAAGUCAUCCAGAUUCGGUA	AC2 and AC3 overlap region
Y35A2	1305	1328	–	24	25629.38	CACCAUCCAAAUACAGUUCAACUA	AC2 and AC3 overlap region
Y35A3	1397	1420	+	24	7187.75	AAUCUCCCAGAUAUACACGCCAUU	AC2 and AC3 overlap region
Y35A4	1911	1933	+	24	3135.87	CACAUCGUCUUCCCUGUUCUACUG	AC1 gene
Y35A5	2404	2424	–	22	8395.19	GCAUGUCCUCAUCCAGUUCGAA	AC1 and AC4 overlap region
Y35A6	785	806	–	22	63853.45	AACAUUCUUCACAGUAGCCGUA	AV1 gene
Y35A7	1091	1112	+	22	4920.27	UUGGUCUACAUAUACAAUGUGU	AC3 gene
Y35A8	1255	1275	–	21	38834.43	AGUGUUUUCUAGUCUACCGAA	AC2 and AC3 overlap region
Y35A9	1284	1305	+	22	8210.77	CCCAGAGCUUUCCGCAGGUUGU	AC2 and AC3 overlap region
Y35A10	1684	1705	–	22	12214.55	UGGAUUGCAGAGAAAGAUAGUG	AC1 gene
Y35A11	1454	1475	+	22	8269.09	GCGUGAAUCCAUGAUCGUGACA	AC2 gene
Y35A12	154	174	+	21	2406.19	CGAGUUUCCCGAAACCGUUCA	AV2 gene
Y35A13	1984	2004	+	21	15961.62	GACGACAUUCUCGGCAGCCCA	AC1 gene
Y35A14	2330	2351	–	22	15721.14	GGUCAGCACAUUUCCAUCCGAA	AC1 and AC4 overlap region
Y35A15	2239	2260	–	22	8474.05	UCUGCAGGGAACUACACGAAGA	AC1 and AC4 overlap region
Y35A16	1726	1749	–	24	34395.38	AAUACAAAGUACGGGAAGCCAGUU	AC1 gene
Y35A17	2586	2606	–	21	4652.19	CAGUCAAUAUGCCUCAGCCAA	AC1 gene
Y35A18	371	392	–	23	2850.82	GGGCAGCAGCACGGCUCACAUAU	AV1 and V2 overlap region
Y35A19	866	886	+	21	2541.24	UGCGUCCAAGGAACAAGCCCU	AV1 gene

AverCov: Average Coverage.

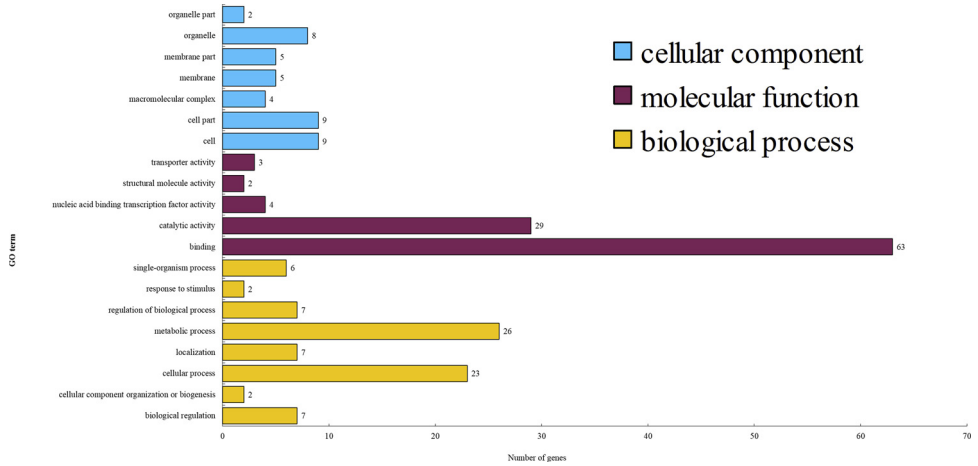

Fig. 5. Gene ontology (GO) classification of predicted *N. benthamiana* target genes of TbCSV- derived siRNAs. They were fallen into three main categories: molecular function; biological process; and cellular component. The number following the term represents the number of targets in this term.

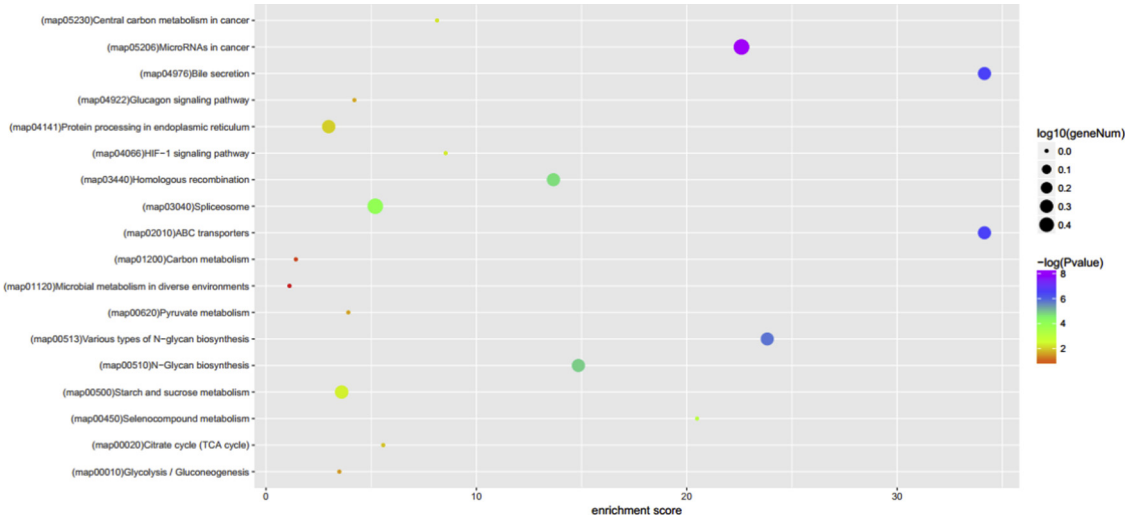

Fig. 6. Kyoto Encyclopedia of Genes and Genomes (KEGG) classification of the predicted *N. benthamiana* target genes of TbCSV- derived siRNAs. The enrichment factor reflects the degree of targets in a given pathway. The number of targets in the pathway is indicated by the circled area, and the circle color represents the ranges of the corrected P-value.

predicted target genes of the vsiRNAs. In total, the 117 target genes were classified into 18 KEGG pathways (Fig. 6). The most represented pathways were “microRNAs in cancer,” “spliceosome”, and “starch and sucrose metabolism.” This suggests that vsiRNAs influence host metabolism by regulating the expression of host genes. Six coding transcripts were selected for RT-qPCR validation based on the finding that their predicted targets were downregulated by vsiRNAs, which putatively were targeted by the 6 vsiRNAs from the viral mRNA. All six genes were downregulated (with a fold change of –1.23 to –4.0), and exhibited significantly decreased expression levels in the TbCSV- infected samples compared to the mock- inoculated control (Fig. 7); however, all 6 genes exhibited no differential expression between TbCSV- and TbCSV + TbCSB- infected plants. These results suggest that these highly expressed vsiRNAs can most likely target specific host genes to promote viral infection.

4. Discussion

During plant viral infection, abundant vsiRNAs are produced from viral dsRNA formed by the imperfect folding of self-complementary sequences within viral ssRNA (Molnar et al., 2005). With the development of sequencing technology, vsiRNA populations have been characterized from a variety of plant viruses with varied resources (Donaire et al., 2008; Li et al., 2016b; Lin et al., 2017; Mallory et al., 2005; Molnar et al., 2005; Qiu et al., 2017; Xia et al., 2014), but the characteristics of plant ssDNA vsiRNAs remain relatively less studied. Furthermore, based on the different symptoms found in TbCSV- and TbCSV + TbCSB- infected plants, we assumed that the virus in each of these two samples may generate diverse vsiRNA profiles in terms of polarity of strand origins, population constitution, distribution hotspots, and pattern in the viral genome. In this study, we showed that TbCSB influenced the expression of TbCSV and the accumulation of vsiRNAs, but it did not affect the characteristics of the vsiRNAs derived from TbCSV.

The production of vsiRNAs requires DCLs, AGOs, and RDRs. DCL2, DCL3, and DCL4 target viral genome in a hierarchical fashion to yield vsiRNAs of 22-, 24-, and 21- nt, respectively (Bouche et al., 2006; Brodersen et al., 2008; Donaire et al., 2008; Garcia-Ruiz et al., 2010). Li et al (2013) analyzed rice black-streaked dwarf virus (RBSDV)-derived vsiRNAs and found that they were predominantly 21- and 22- nt long, were equally derived from both strands. In cucumber green mottle mosaic virus (CGMMV)-infected cucumber plants, 21- and 22- nt vsiRNAs were highly accumulated, and those with a C at their 5′-termini were the most abundant (Li et al., 2016a). Most vsiRNAs from a

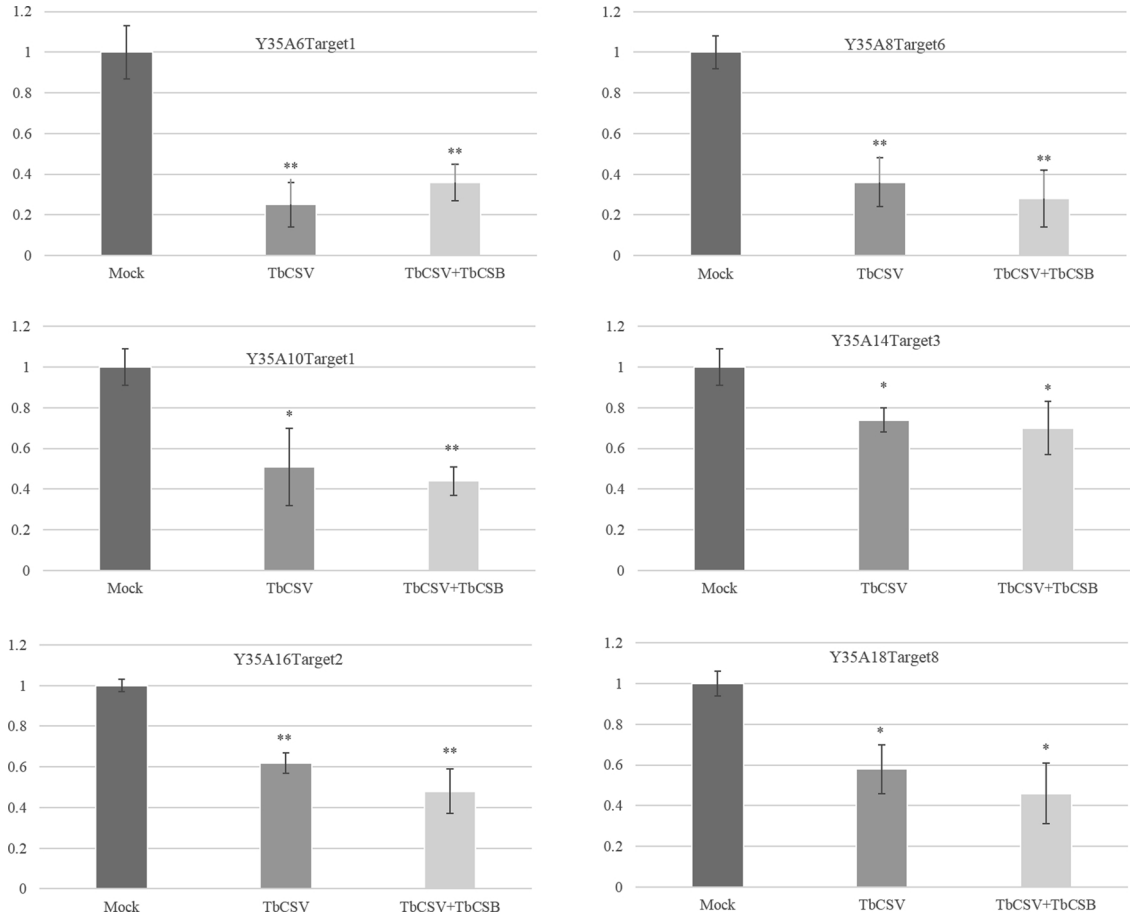

Fig. 7. Expression levels of putative target genes of the vsiRNAs in *N. benthamiana* determined using RT-qPCR. Single and double asterisks indicate significance levels of < 0.05 and < 0.01, respectively.

CMV 2b-deficient mutant in *N. tabacum* were 21- and 22- nt in length, and the 5′-terminal were dominated by A and U (Qiu et al., 2017). VsiRNAs derived from the bipartite circular DNA geminivirus cabbage leaf curl virus (CaLCuV) in *Arabidopsis* were predominantly 21-, 22-, and 24- nt in length (Aregger et al., 2012). In this study, we analyzed the length range of vsiRNAs from TbCSV and TbCSB in infected *N. benthamiana*. Our results showed that most of them were 22- or 21- nt in length, in both TbCSV- and TbCSV + TbCSB- infected plants. These results indicated that 22- and 21- nt vsiRNAs produced by DCL2 and DCL4 are key elements in viral infection, which is consistent with observations made in *N. benthamiana* challenged with other viruses (Aregger et al., 2012; Margaria et al., 2016, 2015; Xu et al., 2012). By contrast, we detected fewer 24- nt vsiRNAs in the two samples, suggesting that DCL3 plays only a minor role in the biogenesis of TbCSV-specific siRNAs in *N. benthamiana*.

Previous studies have indicated that the 5′-terminal nucleotides of vsiRNAs play a pivotal role in directing vsiRNAs to specific AGOs (Mi et al., 2008). A clear preference for A as the 5′-terminal nucleotide was observed, which was indicative of high binding affinity for AGO2 and AGO4 homologs (Donaire et al., 2009; Lin et al., 2017). However, a bias for sequences beginning with a 5′-C suggests a high binding affinity of AGO5 homologs (Donaire et al., 2009; Mi et al., 2008). We also found a greater number of vsiRNAs with U or A at the 5′- terminus than C or G. This demonstrates that AGO1 and AGO2 play important roles during TbCSV infection in *N. benthamiana*. Additionally, the 5′-terminal base of vsiRNAs was biased to U and A, suggesting that vsiRNAs might be loaded into diverse AGOs to disturb the gene expression of virus and host plants. These results suggest that TbCSV- derived vsiRNAs share some similarities with most of the identified plant virus vsiRNAs.

RDRs have been identified in a wide range of plants, and they are essential for the synthesis of dsRNAs, which are eventually cleaved into small RNAs that participate in RNA silencing (Qi et al., 2009; Voinnet, 2009; Wang et al., 2010). It has been shown that *RDR1* and *RDR6* play important roles in viral infection and take part in the biogenesis of secondary vsiRNAs. Several researchers have reported that *RDR1* is associated with the accumulation of viral RNAs, which is induced by viral infection or salicylic acid (SA) treatment (Liao et al., 2015; Yu et al., 2003). Transgenic *NtRDR*1-expressing plants accumulate more viral RNA and develop symptoms in both inoculated leaves and upper uninoculated leaves (Xie et al., 2001). *NbRDR1m*, an *RDR1* homolog, contains a 72-nt insertion in the 5′ region of the ORF, and could be induced by SA and TMV infection (Yang et al., 2004). Furthermore, Wylie et al. (2015) there was no difference between *NbRDR1* and *NbRDR1m* plants in terms of susceptibility to the tested viruses (yellow tailflower mild mottle virus isolate Cervantes, bean yellow mosaic virus isolate SW3.2, CMV isolate SW-11, and tomato spotted wilt virus isolte WA-7), as defined by the ability of the virus to infect the plant systemically. In our studies, we proposed that the high *NbRDR1m* expression in the TbCSV + TbCSB sample leads to the promotion of virus accumulation. Previous reports showed that *RDR6* plays a tissue-specific role in the inhibition of Chinese wheat mosaic virus (CWMV) accumulation and vsiRNA biogenesis at higher temperatures (Andika et al., 2013). In this study, we showed that TbCSV and TbCSB did not influence the expression of *NbRDR6*. This result was similar to previous reports, which showed that the majority of primary vsiRNAs accumulating during infection by the geminivirus CaLCuV were RDR1/2/6-independent, and that geminiviral mRNAs appear to be poor templates for RDR-dependent production of secondary vsiRNAs (Aregger et al.,

2012). However, compared to viral infection in wild-type plants, the disease development was faster and the accumulation of viruses was higher in the *RDR6*-silenced plants (Additional file 6: Figure S3). These results indicate that *RDR6* affects the infection of TbCSV, which is similar to the results reported for many other plant viruses, but the mechanism needs further study.

The RNAi-mediated silencing of gene expression functions on the principle of sequence complementarity irrespective of the origin of the transcripts. Researchers have shown that some of vsiRNAs could regulate host genes by exploiting the RNA-silencing mechanism to enhance their infection and influence host pathogenesis. TMV-derived siRNAs were revealed to target host mRNAs involved in RNA processing and defense response in the host (Qi et al., 2009). Small RNAs from sugarcane mosaic virus (SCMV) target maize mRNAs involved in ribosome biogenesis and other biotic and abiotic stress-related pathways (Xia et al., 2014). Furthermore, vsiRNAs from CMV target many host genes, which, based on KEGG analysis, participate in metabolic processes, cellular processes, and single-organism processes and, based on GO annotation, are related to metabolic activities. These results indicate that some of vsiRNAs involved in the development of disease symptoms (Qiu et al., 2017). Moreover, vsiRNAs derived from plant viroids also have this function. For instance, potato spindle tuber viroid (PSTVd)-derived vsiRNAs may silence two callose synthase genes and greatly affect the disease severity and accumulation of viroids, and peach latent mosaic viroid (PLMVd)-derived siRNAs target the chloroplastic heat shock protein 90 gene in peach to induce albinism and potentially create a favorable host environment for viroid infection (Adkar-Purushothama et al., 2015; Navarro et al., 2012). Furthermore, vsiRNAs from DNA viruses have been documented in plants. Chellappan et al (2004) showed that geminiviruses were able to trigger PTGS by producing two classes of vsiRNAs in *N. benthamiana* and cassava, but this pathway was dependent on the intrinsic features of the virus and the interaction with host plant. VsiRNAs derived from cauliflower mosaic virus (CaMV) target host genes and induce their expression (Moissiard and Voinnet, 2006). In our study, we identified 19 vsiRNAs from TbCSV that potentially target host genes involved in different processes and pathways. Moreover, the functional annotation of these target transcripts of TbCSV siRNA revealed the enrichment of transmembrane transport in the biological process category, membrane in the cellular component category, and active transmembrane transporter activity in the molecular function category. These results suggest that vsiRNAs derived from TbCSV can participate in degrading complementary cellular transcripts to create cellular conditions suitable for viral infection. Analysis of the vsiRNA will lead to a better understanding of the interaction between TbCSV and TbCSB, and the interaction between host and virus.

5. Conclusions

VsiRNAs derived from TbCSV- infected *N. benthamiana* were characterized. Additionally, the effects of TbCSB on the production of vsiRNAs was analyzed. The annotated genes targeted by the vsiRNAs were found to be involved in molecular functions and biological processes. These findings highlight the importance of a deeper understanding of the role of vsiRNAs on viral replication, pathogenicity, and host machinery. This study also furthers our understanding of virus-host interactions.

Author contributions

Ling Qing, and Gentu Wu conceived and designed the study, and revised the paper. Gentu Wu, Qiao Hu, Jiang Du, Ke Li, and Chenchen Jing performed the experiments, Miao Sun, Mingjun Li, and Junmin Li analyzed the data. Gentu Wu, and Ling Qing participated in the manuscript preparation, including the discussion and editing. All authors read and approved the final manuscript.

Consent for publication

All the authors consent to publish.

Compliance with ethical standards

This article does not contain any experiments with human participants or animals performed by any of the authors and is in compliance with ethical standards for research.

Research involving human and animals rights

No human or animal subjects were used in this study.

Informed consent

No human subjects were used in this study.

Funding

This research was supported financially by the China Postdoctoral Science Foundation (Grant No. 2015M572431), Chongqing Postdoctoral Science special Foundation (Grant No. Xm2015120), National Natural Science Founding of China (Grant No. 31772127), and Fundamental Research Funds for the Central Universities (Grant No. XDJK2017A006).

Conflicting interests

The authors declare that they have no conflicts of interest with respect to the data, authorship, or publication of this article.

Acknowledgments

We are grateful to Professor Xueping Zhou in the Biotechnology Institute of Zhejiang University for providing the infectious clones of TbCSV isolate Y35 (Y35 A) and its β satellite (Y35B). We also very thanks to Fei Yan of the Ningbo Universiyt, Ningbo, China, and Jinping Zhao of Texas A&M University AgriLife Research Center, Dallas, USA, correcting the English in the manuscript.

Appendix A. Supplementary data

Supplementary material related to this article can be found, in the online version, at doi:https://doi.org/10.1016/j.virusres.2019.02.017.

References

Adkar-Purushothama, C.R., Brosseau, C., Giguere, T., Sano, T., Moffett, P., Perreault, J.P., 2015. Small RNA derived from the virulence modulating region of the potato spindle tuber viroid silences callose synthase genes of tomato plants. Plant Cell 27 (8), 2178–2194.

Andika, I.B., Sun, L.Y., Xiang, R., Li, J.M., Chen, J.P., 2013. Root-specific role for *Nicotiana benthamiana* RDR6 in the inhibition of Chinese wheat mosaic virus accumulation at higher temperatures. Mol. Plant Microbe. Interact 26 (10), 1165–1175.

Aregger, M., Borah, B.K., Seguin, J., Rajeswaran, R., Gubaeva, E.G., Zvereva, A.S., Windels, D., Vazquez, F., Blevins, T., Farinelli, L., Pooggin, M.M., 2012. Primary and secondary siRNAs in geminivirus-induced gene silencing. PLoS Pathog 8 (9) e1002941.

Bouche, N., Lauressergues, D., Gasciolli, V., Vaucheret, H., 2006. An antagonistic function for Arabidopsis DCL2 in development and a new function for DCL4 in generating viral siRNAs. EMBO J 25 (14), 3347–3356.

Brodersen, P., Sakvarelidze-Achard, L., Bruun-Rasmussen, M., Dunoyer, P., Yamamoto, Y.Y., Sieburth, L., Voinnet, O., 2008. Widespread translational inhibition by plant miRNAs and siRNAs. Science 320 (5880), 1185–1190.

Byrne, M.E., 2012. Making leaves. Curr. Opin. Plant Biol. 15 (1), 24–30.

Chellappan, P., Vanitharani, R., Pita, J., Fauquet, C.M., 2004. Short interfering RNA accumulation correlates with host recovery in DNA virus-infected hosts, and gene silencing targets specific viral sequences. J. Virol 78 (14), 7465–7477.

Csorba, T., Kontra, L., Burgyan, J., 2015. Viral silencing suppressors: tools forged to fine-tune host-pathogen coexistence. Virology 479-480, 85–103.

Deng, Y.T., Wang, J.B., Tung, J., Liu, D., Zhou, Y.J., He, S., Du, Y.L., Baker, B., Li, F., 2018. A role for small RNA in regulating innate immunity during plant growth. PLoS Pathog 14 (1) e1006756.
Ding, C.J., Qing, L., Li, Z.H., Liu, Y., Qian, Y.J., Zhou, X.P., 2009. Genetic determinants of symptoms on viral DNA satellites. Appl. Environ. Microbiol 75 (16), 5380–5389.
Donaire, L., Barajas, D., Martinez-Garcia, B., Martinez-Priego, L., Pagan, I., Llave, C., 2008. Structural and genetic requirements for the biogenesis of tobacco rattle virus-derived small interfering RNAs. J. Virol. 82 (11), 5167–5177.
Donaire, L., Wang, Y., Gonzalez-Ibeas, D., Mayer, K.F., Aranda, M.A., Llave, C., 2009. Deep-sequencing of plant viral small RNAs reveals effective and widespread targeting of viral genomes. Virology 392 (2), 203–214.
Fang, X.F., Qi, Y.J., 2016. RNAi in plants: an argonaute-centered view. Plant Cell 28 (2), 272–285.
Garcia-Ruiz, H., Takeda, A., Chapman, E.J., Sullivan, C.M., Fahlgren, N., Brempelis, K.J., Carrington, J.C., 2010. Arabidopsis RNA-dependent RNA polymerases and dicer-like proteins in antiviral defense and small interfering RNA biogenesis during *Turnip mosaic virus* infection. Plant Cell 22 (2), 481–496.
Hamilton, A.J., Baulcombe, D.C., 1999. A species of small antisense RNA in post-transcriptional gene silencing in plants. Science 286 (5441), 950–952.
Jaubert, M., Bhattacharjee, S., Mello, A.F., Perry, K.L., Moffett, P., 2011. ARGONAUTE2 mediates RNA-silencing antiviral defenses against *Potato virus X* in *Arabidopsis*. Plant Physiol. 156 (3), 1556–1564.
Li, Z.H., Xie, Y., Zhou, X.P., 2005. *Tobacco curly shoot virus* DNAbeta is not necessary for infection but intensifies symptoms in a host-dependent manner. Phytopathology 95 (8), 902–908.
Li, J.M., Andika, I.B., Shen, J.F., Lv, Y.D., Ji, Y.Q., Sun, L.Y., Chen, J.P., 2013. Characterization of *Rice black-streaked dwarf virus*- and *Rice stripe virus*-derived siRNAs in singly and doubly infected insect vector *Laodelphax striatellus*. PLoS One 8 (6) e66007.
Li, J.M., Zheng, H.Y., Zhang, C.C., Han, K.L., Wang, S., Peng, J.J., Lu, Y.W., Zhao, J.P., Xu, P., Wu, X.H., Li, G.J., Chen, J.P., Yan, F., 2016a. Different virus-derived siRNAs profiles between leaves and fruits in *Cucumber green mottle mosaic virus*-infected Lagenaria siceraria plants. Front. Microbiol. 7, 1797.
Li, Y.Q., Deng, C.L., Shang, Q.X., Zhao, X.L., Liu, X.L., Zhou, Q., 2016b. Characterization of siRNAs derived from *Cucumber green mottle mosaic virus* in infected cucumber plants. Arch. Virol 161 (2), 455–458.
Liao, Y.W., Liu, Y.R., Liang, J.Y., Wang, W.P., Zhou, J., Xia, X.J., Zhou, Y.H., Yu, J.Q., Shi, K., 2015. The relationship between the plant-encoded RNA-dependent RNA polymerase 1 and alternative oxidase in tomato basal defense against Tobacco mosaic virus. Planta 241 (3), 641–650.
Lin, W.W., Yan, W.K., Yang, W.T., Yu, C.W., Chen, H.H., Zhang, W., Wu, Z.J., Yang, L., Xie, L.H., 2017. Characterisation of siRNAs derived from new isolates of *Bamboo mosaic virus* and their associated satellites in infected ma bamboo (*Dendrocalamus latiflorus*). Arch. Virol 162 (2), 505–510.
Mallory, A.C., Bartel, D.P., Bartel, B., 2005. MicroRNA-directed regulation of Arabidopsis AUXIN RESPONSE FACTOR17 is essential for proper development and modulates expression of early auxin response genes. Plant Cell 17 (5), 1360–1375.
Mansoor, S., Briddon, R.W., Zafar, Y., Stanley, J., 2003. Geminivirus disease complexes: an emerging threat. Trends Plant Sci 8 (3), 128–134.
Margaria, P., Miozzi, L., Rosa, C., Axtell, M.J., Pappu, H.R., Turina, M., 2015. Small RNA profiles of wild-type and silencing suppressor-deficient *Tomato spotted wilt virus* infected *Nicotiana benthamiana*. Virus Res 208, 30–38.
Margaria, P., Miozzi, L., Ciuffo, M., Rosa, C., Axtell, M.J., Pappu, H.R., Turina, M., 2016. Comparison of small RNA profiles in *Nicotiana benthamiana* and *Solanum lycopersicum* infected by polygonum ringspot tospovirus reveals host-specific responses to viral infection. Virus Res 211, 38–45.
Mi, S.J., Cai, T., Hu, Y.G., Chen, Y.M., Hodges, E., Ni, F.R., Wu, L., Li, S., Zhou, H.Y., Long, C.G., Chen, S., Hannon, G.J., Qi, Y.J., 2008. Sorting of small RNAs into *Arabidopsis* argonaute complexes is directed by the 5' terminal nucleotide. Cell 133 (1), 116–127.
Miozzi, L., Gambino, G., Burgyan, J., Pantaleo, V., 2013. Genome-wide identification of viral and host transcripts targeted by viral siRNAs in Vitis vinifera. Mol. Plant Pathol 14 (1), 30–43.
Moissiard, G., Voinnet, O., 2006. RNA silencing of host transcripts by *Cauliflower mosaic virus* requires coordinated action of the four Arabidopsis Dicer-like proteins. Proc. Natl. Acad. Sci. U. S. A. 103 (51), 19593–19598.
Molnar, A., Csorba, T., Lakatos, L., Varallyay, E., Lacomme, C., Burgyan, J., 2005. Plant virus-derived small interfering RNAs originate predominantly from highly structured single-stranded viral RNAs. J. Virol. 79 (12), 7812–7818.
Moyo, L., Ramesh, S.V., Kappagantu, M., Mitter, N., Sathuvalli, V., Pappu, H.R., 2017. The effects of *Potato virus Y*-derived virus small interfering RNAs of three biologically distinct strains on potato *(Solanum tuberosum)* transcriptome. Virol. J. 14 (1), 129.
Navarro, B., Gisel, A., Rodio, M.E., Delgado, S., Flores, R., Di Serio, F., 2012. Small RNAs containing the pathogenic determinant of a chloroplast-replicating viroid guide the degradation of a host mRNA as predicted by RNA silencing. Plant J. 70 (6), 991–1003.
Qi, X.P., Bao, F.S., Xie, Z.X., 2009. Small RNA deep sequencing reveals role for *Arabidopsis thaliana* RNA-dependent RNA polymerases in viral siRNA biogenesis. PLoS One 4 (3) e4971.
Qiu, Y.H., Zhang, Y.J., Hu, F., Zhu, S.F., 2017. Characterization of siRNAs derived from *Cucumber mosaic virus* in infected tobacco plants. Arch. Virol. 162 (7), 2077–2082.
Sha, A.H., Zhao, J.P., Yin, K.Q., Tang, Y., Wang, Y., Wei, X., Hong, Y.G., Liu, Y.L., 2014. Virus-based MicroRNA silencing in plants. Plant Physiol. 164 (1), 36–47.
Shi, B.B., Lin, L., Wang, S., Guo, Q., Zhou, H., Rong, L.L., Li, J.M., Peng, J.J., Lu, Y.W., Zheng, H.Y., Yang, Y., Chen, Z., Zhao, J.P., Jiang, T., Song, B.A., Chen, J.P., Yan, F., 2016. Identification and regulation of host genes related to *Rice stripe virus* symptom production. New Phytol 209 (3), 1106–1119.
Shimura, H., Pantaleo, V., Ishihara, T., Myojo, N., Inaba, J., Sueda, K., Burgyan, J., Masuta, C., 2011. A viral satellite RNA induces yellow symptoms on tobacco by targeting a gene involved in chlorophyll biosynthesis using the RNA silencing machinery. PLoS Pathog 7 (5) e1002021.
Shivaprasad, P.V., Chen, H.M., Patel, K., Bond, D.M., Santos, B.A., Baulcombe, D.C., 2012. A microRNA superfamily regulates nucleotide binding site-leucine-rich repeats and other mRNAs. Plant Cell 24 (3), 859–874.
Smith, N.A., Eamens, A.L., Wang, M.B., 2011. Viral small interfering RNAs target host genes to mediate disease symptoms in plants. PLoS Pathog. 7 (5) e1002022.
Tao, X.R., Zhou, X.P., 2008. Pathogenicity of a naturally occurring recombinant DNA satellite associated with tomato yellow leaf curl China virus. J. Gen. Virol. 89 (Pt 1), 306–311.
Teotia, S.C., Tang, G.L., 2015. To bloom or not to bloom: role of microRNAs in plant flowering. Mol. Plant 8 (3), 359–377.
Tong, A.Z., Yuan, Q., Wang, S., Peng, J.J., Lu, Y.W., Zheng, H.Y., Lin, L., Chen, H.R., Gong, Y.F., Chen, J.P., Yan, F., 2017. Altered accumulation of osa-miR171b contributes to *Rice stripe virus* infection by regulating disease symptoms. J. Exp. Bot 68 (15), 4357–4367.
Voinnet, O., 2009. Origin, biogenesis, and activity of plant microRNAs. Cell 136 (4), 669–687.
Wang, X.B., Wu, Q., Ito, T., Cillo, F., Li, W.X., Chen, X., Yu, J.L., Ding, S.W., 2010. RNAi-mediated viral immunity requires amplification of virus-derived siRNAs in Arabidopsis thaliana. Proc. Natl. Acad. Sci. U. S. A. 107 (1), 484–489.
Wang, S., Cui, W.J., Wu, X.Y., Yuan, Q., Zhao, J.P., Zheng, H.Y., Lu, Y.W., Peng, J.J., Lin, L., Chen, J.P., Yan, F., 2018. Suppression of nbe-miR166h-p5 attenuates leaf yellowing symptoms of potato virus X on *Nicotiana benthamiana* and reduces virus accumulation. Mol. Plant Pathol. 19 (11), 2384–2396.
Wylie, S.J., Zhang, C., Long, V., Roossinick, M.J., Koh, S.H., Jones, K.G.K., Iqbal, S., Li, H., 2015. Differential responses to virus challenge of laboratory and wild accessions of Australian species of *Nicotiana*, and comparative analysis of RDR1 gene sequences. PLoS One 10 (3) e0121787.
Xia, Z.H., Peng, J., Li, Y.Q., Chen, L., Li, S., Zhou, T., Fan, Z.F., 2014. Characterization of small interfering RNAs derived from *Sugarcane mosaic virus* in infected maize plants by deep sequencing. PLoS One 9 (5) e97013.
Xie, Z.X., Fan, B.F., Chen, C.H., Chen, Z.X., 2001. An important role of an inducible RNA-dependent RNA polymerase in plant antiviral defense. Proc. Natl. Acad. Sci. U. S. A. 98 (11), 6516–6521.
Xie, K.B., Wu, C.Q., Xiong, L.Z., 2006. Genomic organization, differential expression, and interaction of SQUAMOSA promoter-binding-like transcription factors and microRNA156 in rice. Plant Physiol. 142 (1), 280–293.
Xu, Y., Huang, L.Z., Fu, S., Wu, J.X., Zhou, X.P., 2012. Population diversity of *Rice stripe virus*-derived siRNAs in three different hosts and RNAi-based antiviral immunity in *Laodelphgax striatellus*. PLoS One 7 (9) e46238.
Xu, D.L., Zhou, G.H., 2017. Characteristics of siRNAs derived from *Southern rice black-streaked dwarf virus* in infected rice and their potential role in host gene regulation. Virol. J. 14 (1), 27.
Yang, S.J., Carter, S.A., Cole, A.B., Cheng, N.H., Nelson, R.S., 2004. A natural variant of a host RNA-dependent RNA polymerase is associated with increased susceptibility to viruses by Nicotiana benthamiana. Proc. Natl. Acad. Sci. U. S. A. 101 (16), 6297–6302.
Yin, K.Q., Tang, Y., Zhao, J.P., 2015. Genome-wide characterization of miRNAs involved in N Gene-mediated immunity in response to tobacco mosaic virus in Nicotiana benthamiana. Evol. Bioinform. 11 (S1), 1–11.
Yu, D., Fan, B., MacFarlane, S.A., Chen, Z., 2003. Analysis of the involvement of an inducible *Arabidopsis* RNA-dependent RNA polymerase in antiviral defense. Mol. Plant Microbe. Interact. 16 (3), 206–216.
Zhu, H., Duan, C.G., Hou, W.N., Du, Q.S., Lv, D.Q., Fang, R.X., Guo, H.S., 2011. Satellite RNA-derived small interfering RNA satsiR-12 targeting the 3' untranslated region of *Cucumber mosaic virus* triggers viral RNAs for degradation. J. Virol. 85 (24), 13384–13397.